Heliyon 6 (2020) e03366

Contents lists available at ScienceDirect

Heliyon

journal homepage: www.cell.com/heliyon

Research article

Fatigue life of underwater wet welded low carbon steel SS400

N. Muhayat [a], Y.A. Matien [a], H. Sukanto [a], Y.C.N. Saputro [b], Triyono [a,*]

[a] Mechanical Engineering Department, Sebelas Maret University, Surakarta, Indonesia
[b] UPTB Solo Technopark, Technical Unit on Regional Development Planning Board Surakarta, Indonesia

ARTICLE INFO

Keywords:
Materials science
Mechanical engineering
Underwater
Wet welding
Fatigue life
Low carbon steel
Water depth
Acicular ferrite

ABSTRACT

Underwater welding is widely used for maintenance and repairs of underwater structures such as undersea pipes, offshore structures and nuclear power plants. In practice, underwater welding has the disadvantage related to high cooling rate and unstable welding arc due to the water hydrostatic pressure. This affects the microstructure and mechanical properties of underwater welded joints. Many of previous research works on underwater welding have been carried out only on a laboratory scale in shallow water depth, whereas underwater welding was used to weld in the depth of the water with a metre scale. Undersea structures experience fatigue load due to the fluctuation force of water flow. Therefore, this study aims to determine the effect of water depth on the fatigue life of underwater welded joints. Low carbon steel SS400 specimens were welded underwater with depths of 2.5 m, 5 m and 10 m. The air welded joint was also evaluated for comparison purposes. Fatigue life was evaluated according to the ASTM E466 standard by using a rotary bending machine. Furthermore, tensile test, micro hardness measurement and microstructure evaluation were also conducted for gathering supporting data. The fatigue and tensile strength of the air welded joints were higher than those of the underwater welded joints. The porosities caused by the dissolved hydrogen gas, carbon (monoxide and dioxide) gases and water vapor in weld metal of the underwater welded joints decreased the fatigue and tensile strength. An interesting phenomenon on the underwater welded joints was that the deeper the water level, the higher became the fatigue, tensile strength as well as hardness. Based on the microstructure analysis, the number of acicular ferrite structures in weld metal increased as the water level depth increased.

1. Introduction

The use of underwater welding applications for the maintenance of underwater structures and marine applications has increased significantly in recent years. Underwater welding is useful in facilitating maintenance and repairs of subsea construction, pipes, marine applications, nuclear power plant, offshore and port structures [1, 2]. Underwater welding is categorised into dry and wet underwater welding. The wet underwater welding is widely used due to the operating cost, which is lower compared to dry underwater welding. However, the wet underwater welding technique possesses a high cooling rate as the weld metal and welding arc are in straight contact with water [3]. The high cooling rate of wet underwater welding drives the creation of a martensitic structure that impacts the weld metal's fatigue resistance [4]. Besides the cooling rate, a drawback of underwater weld is the unsteady arc of electrodes in the course of welding because of the hydrostatic pressure of water, and hence its penetration is not as good as the air welding [5].

The drawbacks of underwater welding impact the mechanical and microstructure properties of the welded joint. The weld metal of underwater welding is regulated by martensite structure whose toughness is lower as against weld metal which is regulated by ferrite structure [6]. Furthermore, the hardness of underwater welded joints is greater compared to that of air welded joints [7]. Fatigue testing on underwater welded joints is quite crucial, as the welded joints are subjected to cyclic loading because of the water waves which cause cracks, thereby reducing fatigue resistance of the weld joint. Data on fatigue resistance of underwater weld joints is still inadequate. Recently, underwater welding studies have carried out evaluation only using impact, tensile strength, and hardness tests. In addition, previous underwater welding studies have been carried out only on a laboratory scale at shallow water depths [8] or simulated water depth [9], whereas underwater welding applications are for water depths with a meter scale. From the above, a study aiming to determine the fatigue resistance of the underwater welded joints with deeper water levels is significant. Water depth will cause changes in hydrostatic pressure and cooling rate. Hydrostatic pressure

* Corresponding author.
E-mail address: triyonomesin@uns.ac.id (Triyono).

https://doi.org/10.1016/j.heliyon.2020.e03366
Received 22 November 2019; Received in revised form 13 January 2020; Accepted 3 February 2020

will affect the stability of the weld arc, while the cooling rate will affect the microstructure and mechanical properties of the weld metal [3, 10]. The water used in this study is ordinary water which does not flow and is not salty. Welding under flow and salty water will be the next research challenge because the flow and salty water will give different effects from the effects of ordinary water.

2. Experimentals procedure

2.1. Materials preparation and welding process

Cylindrical low carbon steel SS 400 with a diameter of 18 mm was used as research material in this study. Its chemical composition is shown in Table 1. Five specimens for tensile and three specimens fatigue tests were prepared according to ASTM E-8 and ASTM E466 standards, respectively, as illustrated in Figures 1 and 2. Single V groove with groove angle and gap distance of 70° and 1 mm respectively was used. A gap distance of 1 mm aims to improve the penetration. KOBEWEL KA-602 Shielded Metal Arc Welding (SMAW) machine was used for underwater weld. Underwater welds were performed in water depths of 2.5, 5 and 10 m, as shown in Figure 3. The air welded joint was also evaluated for comparison. Both underwater and air welding process used E6014 electrode with diameter of 3.2 mm and constant weld current of 90 A.

2.2. Underwater welded joint characterisation

Macrostructure and microstructure observations were carried out using Euromex optical microscopy. The standard procedure for microstructure observation including cutting, mounting, polishing and etching was conducted. The etching solution was 80% alcohol, 10% HCl and 10% NHO_3. The observed areas were base metal, heat affected zone (HAZ) and weld metal.

Hardness of welded joints was measured using Highwood micro Vickers tester with a load of 1000 g. The distance of each measuring point in the weld metal area and HAZ was 0.25 mm, while that in the base metal area was 1 mm.

SANS Universal testing machine with a capacity of 10 tons was used to perform tensile tests. Five tensile test specimens were used for each water depth variation. The shape of the welded tensile test specimen is shown in Figure 4.

The SHIMADZU rotary bending machine was used to evaluate the fatigue life of the underwater welded joints. It is driven by an electric motor with a maximum rotational speed of 2850 rpm (Figure 5). Six levels of fatigue load – 60% UTS, 55% UTS, 50% UTS, 45% UTS, 40% UTS and 35% UTS – were selected and subjected to fatigue specimens. The selected load and the fracture cycle number were noted and then plotted to form S–N curve (Wohler diagram). The shape of the welded fatigue test specimen is shown in Figure 6.

3. Result and discussion

3.1. Macrostructure and microstructure

The macrostructure observation is important to identify cracks, porosities, slag and small-scale holes. Based on the macro structure observations, all welded joints, both the air and underwater welded joints, had lacked fussion due to lack of penetration. In contrast to the air welded joint (Figure 7(a)), all the underwater welded joints of 2.5, 5 and 10 m

Tabel 1. Chemical composition of low carbon steel SS400.

Unsur	Fe	C	Si	Mn	P	Cr	Co	Cu
(%)	99.0	0.0139	0.112	0.312	0.0306	0.275	0.0228	0.0200

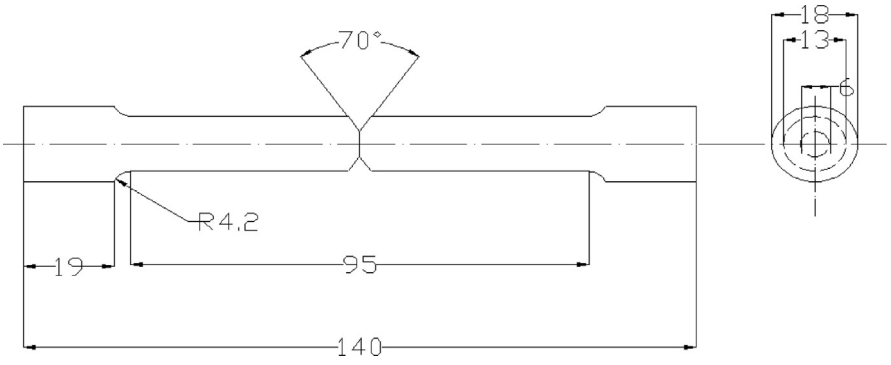

Figure 1. Tensile test specimen based on the ASTM E-8 standard (unit in mm).

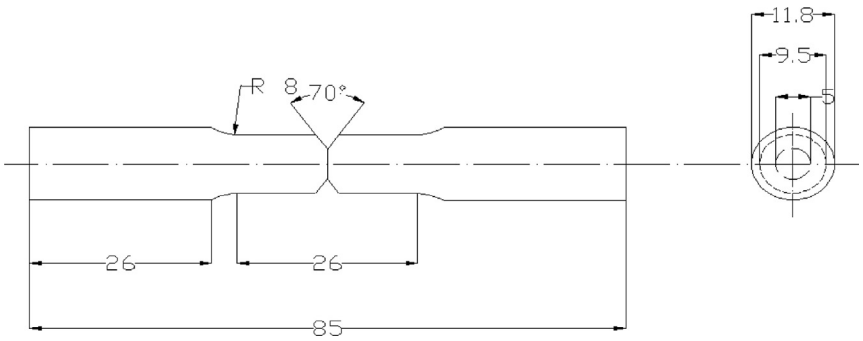

Figure 2. Fatigue test specimen based on the ASTM E-466 standard (unit in mm).

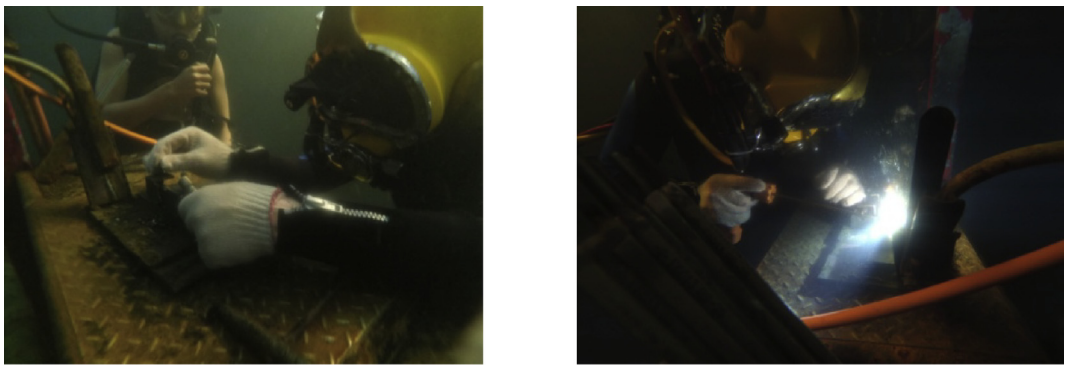

Figure 3. Underwater welding (a) preparation (b) process.

Figure 4. Tensile test specimen.

Figure 5. Rotary bending fatigue test.

Figure 6. Fatigue test specimen.

depth had porosities, as shown in Figures 7(b), 7(c) and 7(d). Porosities were generated by the dissolved hydrogen gas, carbon (monoxide and dioxide) gases and water vapor trapped in the weld metal during the welding process because of the molten metal experienced direct contact with water [10, 11].

The microstructure of base metal is ferrite and pearlite, as shown in Figure 8(a). It is the nature of low carbon steel. The structure of ferrite has a lower tensile strength and hardness compared to the pearlite structure [12]. The microstructure in the weld metal of the air welded joint, shown in Figure 8 (b), is dominated by the polygonal ferrite (PF) and grain boundary ferrite (GBF) phases. The microstructure of the underwater weld metal in 2.5 m depth (Figure 8 (c)) was almost the same as the air weld metal which was dominated by the GBF and PF, but the acicular ferrite (AF) structure also began to appear. The weld metal of the underwater welded joints at 5 and 10 m had different microstructures from that at 2.5 m, as shown in Figures 8 (d) and 8 (e). They were

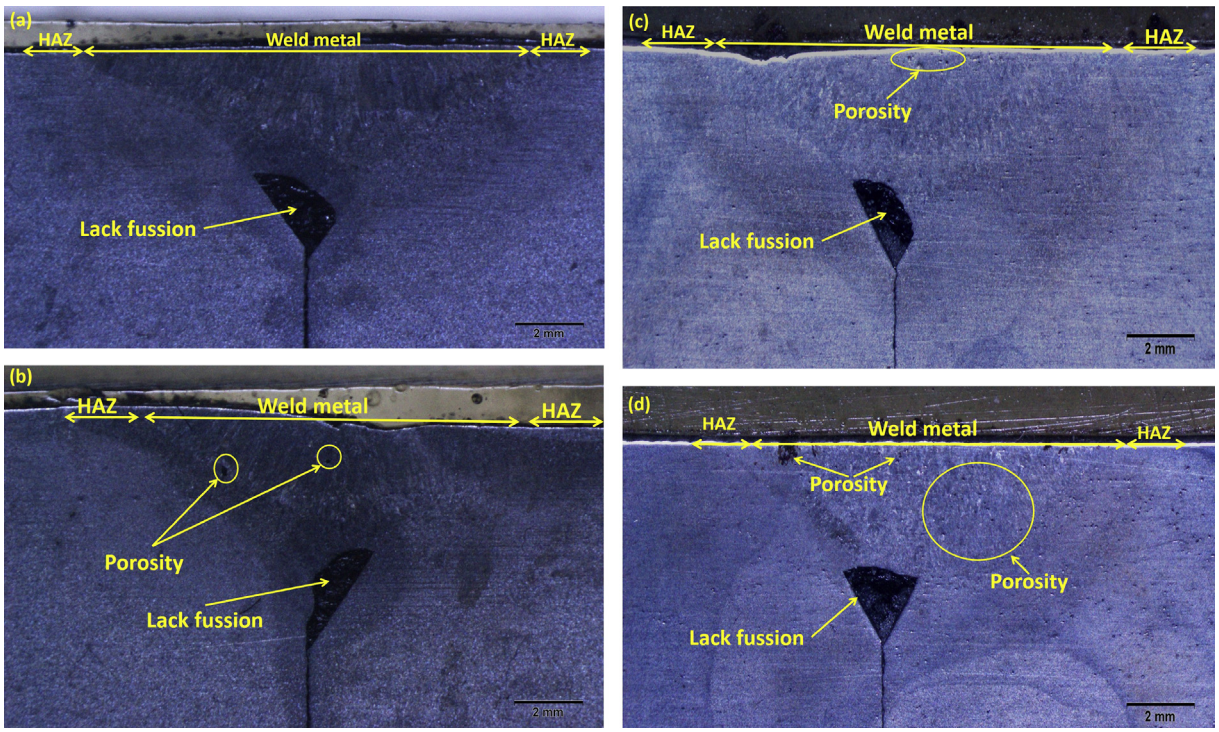

Figure 7. Macrostructure of weld metal (a) air weld (b) underwater weld in depth of 2.5 m (c) underwater weld in depth of 5 m (d) underwater weld in depth of 10 m.

dominated by AF and ferrite with second phase aligned (FSP). The phase transformation of welded steel depends on the carbon content and cooling rate and can be predicted by a continuous cooling transformation (CCT) diagram. Based on the CCT diagram of 0.013%C steel shown in Figure 9, due to the rapid cooling rate, it can be predicted that the formed microstructure in the weld metal of underwater welded steel is AF. The measured water temperatures during welding in depths of 2.5 and 10 m were 29 °C and 24 °C, respectively. It means that the cooling rate at 10 m was higher than that at 2.5 m. According to Di et al. [3] and Zhang et al. [4], the high cooling rate will increase AF phase content in weld metal. Each phase in the weld metal area has different mechanical properties. AF structure has higher tensile strength than GBF and PF structure. Ferrite with second phase aligned (FSP) has tensile strength as high as AF structure but with low ductility [3, 13]. Generally, all types of ferrite structures have a lower tensile strength than that of bainite structure, but based on the CCT diagram (Figure 9), weld metal in this case has no bainite structure and its mechanical properties depended on the types of ferrite structures.

The microstructure of the HAZ both the underwater and the air welded is almost ferrite and little pearlite structures, as shown in Figure 10. This microstructure is almost simillar to base metal microstructure but its grain size is different. HAZ is the area of base metal which is not melted but its microstructure and properties altered by the thermal cycle of welding. The HAZ of the air welded joint has ferrite structure with grain size of 10–20 μm (Figure 10 (a)), while the HAZ of the underwater welded joints at 2.5 and 5 m have ferrite structure with smaller grain size of 5–10 μm, as shown in Figures 10 (b) and 10 (c). As shown in Figure 10 (d), the HAZ of the underwater welded joint at 10 m shows ferrite structure, as the underwater weld depth increases, with the smallest grain size being 5 μm. The difference in grain size of the HAZ areas of the air welded and underwater welded joint is due to the different recrystallisation processes according to the cooling rate. During welding, HAZ experiences high temperature, turns the ferrite structure into austenite structure and then generates the new crystal of ferrite in the austenite grain boundary during cooling process. In air welding process, cooling rate is low so it allows the ferrite crystal grow and make ferrite with big grain size in the end of transformation. In underwater welding process, cooling rate is high due to water surounding so it does not allow the ferrite crystal grow and make ferrite with small grain size in the end of transformation. The deeper water of underwater welding, the higher cooling rate and the smaller grain size. The small grain size and density make the microstructure finer and result in more number of grains, so that the tensile strength and hardness increase [15]. Microstructure observations generally proved that the deeper the water level in underwater welding the higher is the AF content in the weld metal and the lower is the grain size of HAZ. It made the mechanical properties of the underwater welded joints at 10 m depth is better than those at depth of 5 and 2.5 m.

3.2. Mechanical properties

3.2.1. Hardness

The Micro Vickers hardness distribution is shown in Figure 11. Generally, the hardness profile of the welded joint generally increased from the weld metal to the HAZ and then decreased sharply to the base metal. This hardness profile is in accordance with Zhao et al. [15]. Figure 11 also shows that the 10 m depth underwater welded joint had the highest hardness among all the welded joints, with the average hardness of weld metal being 365 HV. Although there were porosities in weld metal, but because of it had a lot of fine acicular ferrite due to high cooling rate, its hardness was very high. It was even higher than hardness of the air weld metal because of the coarse poligonal ferrite (PF) and grain boundary ferrite (GBF) although there were no porosities. The weld metals of the 2.5 m depth underwater welded joint had the lowest hardness, with the average hardness of weld metal being 249 HV. It had both the porosities and coarse grain boundary ferrite (GBF). Due to the finer GBF, the weld metals hardness of the 5 m depth underwater welded metal was higher than that of the 2.5 m depth underwater welded metal.

The hardness of HAZ was higher than the weld metal hardness, because there was no defects and its microstructure grains were fine. This hardness of HAZ was affected by the grain size of microstructure contained in the area being tested. The grain size of microstructure was affected by the cooling rate during welding process. The cooling rate of HAZ from high to low were 10 m, 5 m, 2.5 m and the air welding process

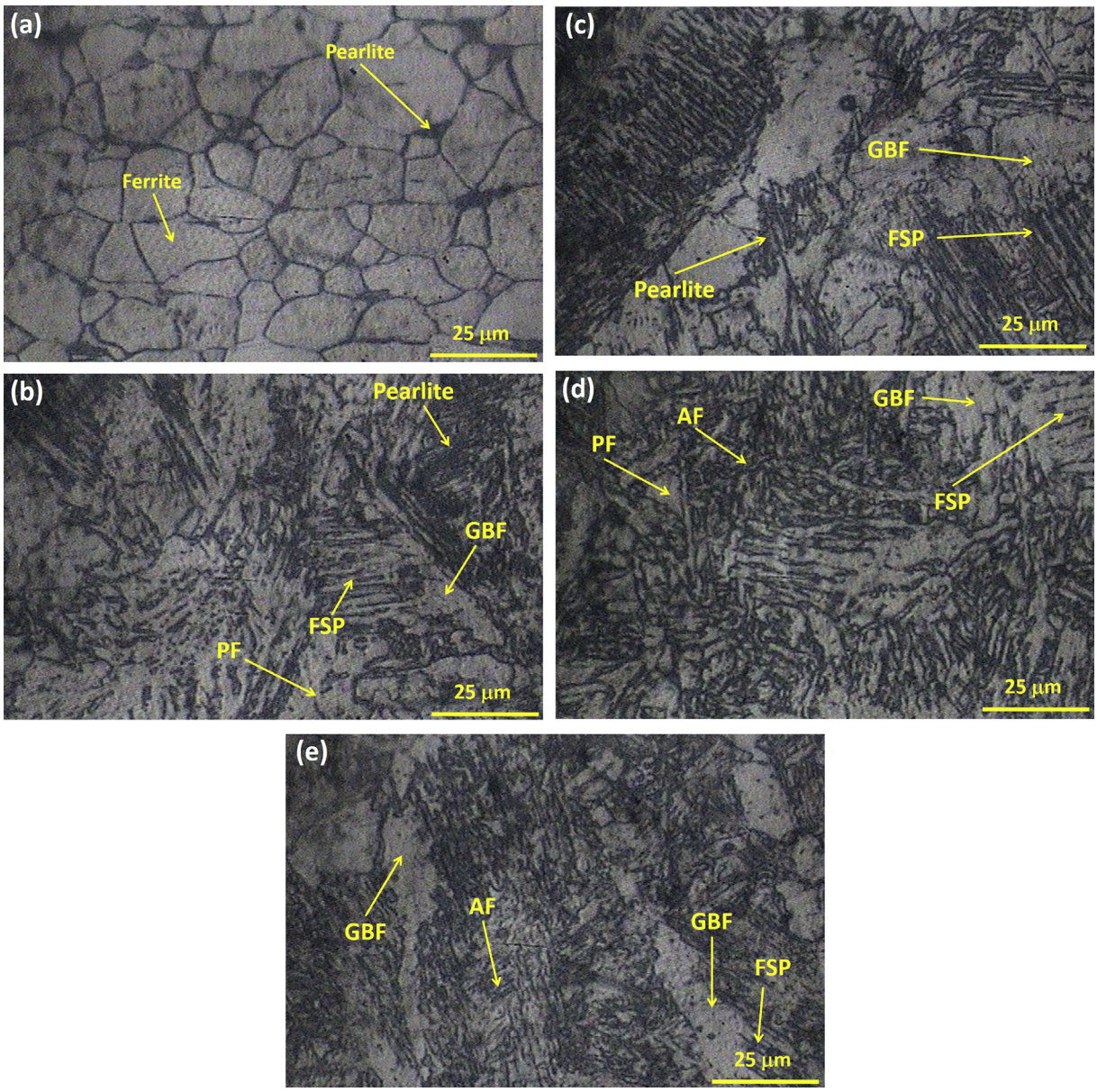

Figure 8. Microstructure of (a) base metal, (b) air weld metal (c) underwater weld in depth of 2.5 m (d) underwater weld in depth of 5 m (e) underwater weld in depth of 10 m.

so the hardness of HAZ from high to low were 10 m, 5 m, 2.5 m and the air welding process. In HAZ, the welding temperature reached the recrystallization temperature which was half the melting point, but it was not too much higher than the recrystallization temperature. Consequently, the time at the recrystallization temperature level was short and not sufficient for the new crystal grains to grow. The new crystal grains became fine and dense, hence increasing the hardness of HAZ. The hardness affected the tensile strength and fatigue resistance [15, 16].

3.2.2. Tensile strength

Figure 12 shows the tensile strength and elongation of the underwater welded joints. Tensile strength of the air welded joint was 365 MPa, whereas that of the underwater welded joints in depths of 2.5, 5 and 10 m was 277, 303 and 313 MPa, respectively. Generally, the tensile strength of underwater welded joints was lower than that of the air welded joint due to the porosities of underwater weld metal. Based on the macro structure, the weld metal of underwater welded joint has porosities because of the solubility of hydrogen in the molten metal. During underwater welding, heat energy of welding electrode not only heated the specimen but also heated the water. Heated water will decompose to give hydrogen and oxygen gasses. These gases will be disolved into molten metal (weld metal) and trapped when it solidified to form porosities. In the case of the underwater welded joints, tensile strength increased with the increase in water depth level. It was influenced by the content of the AF structure in the weld metal of the underwater welded joints. Based on the microstructure discussion, the weld metal of underwater welded joints in 2.5 m water depth had almost grain boundary ferrite (GBF) structures, which were soft and weak, while that in 5 and 10 m water depth had AF and ferrite with second phase aligned (FSP) structures. The increase in AF structure in underwater welded joints of 5 and 10 m water depth was caused by the decrease in water temperature, which ranged from 29 °C at a depth of 2.5 m–24 °C at a depth of 10 m. The decreasing water temperature increased the cooling rate. According to Di et al. [3], increasing the cooling rate increases the amount of AF structures. The increase in the amount of AF structures increases the tensile strength [17]. Another factor that influenced the tensile strength was the grain size. The deeper the water depth of the underwater welded joints, the smaller the grain size of the HAZ. According to Di et al. [3], the smaller

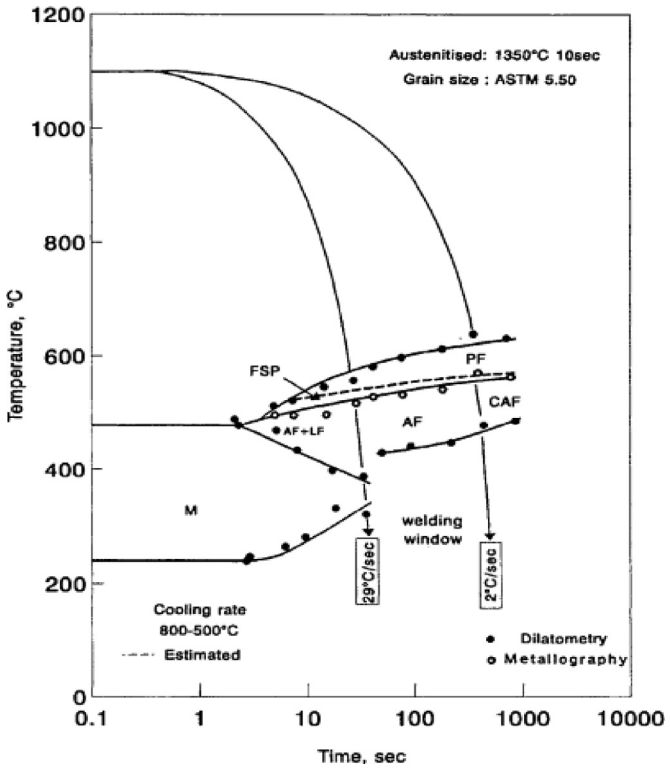

Figure 9. CCT (Continous cooling transformation) diagram of low carbon steel [14].

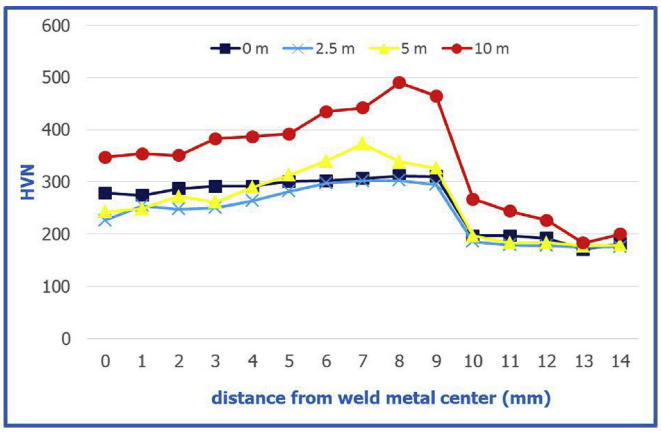

Figure 11. Hardness distribution of weld metal, HAZ and base metal.

grain size increased the tensile strength. In addition to the type and grain size of the micro structure, the hardness of the underwater welded joint also affected the tensile strength. Tensile strength will increase if the hardness of the welded joints increases [13].

The surface fracture of the welded joint tensile test is shown in Figure 13. It shows that both air and underwater welded joints had a mixture of intergranular and transgranular fracture modes. Intergranular fracture was characterised by a rough surface, while transgranular fracture was characterised by a light, smooth and flat surface. These fracture modes are common in low carbon steel fracture [17, 18]. Tensile test fracture surface of underwater welded joints showed porosities, which reduced the tensile strength of the underwater welded joint and made it lower than that of the air welded joint.

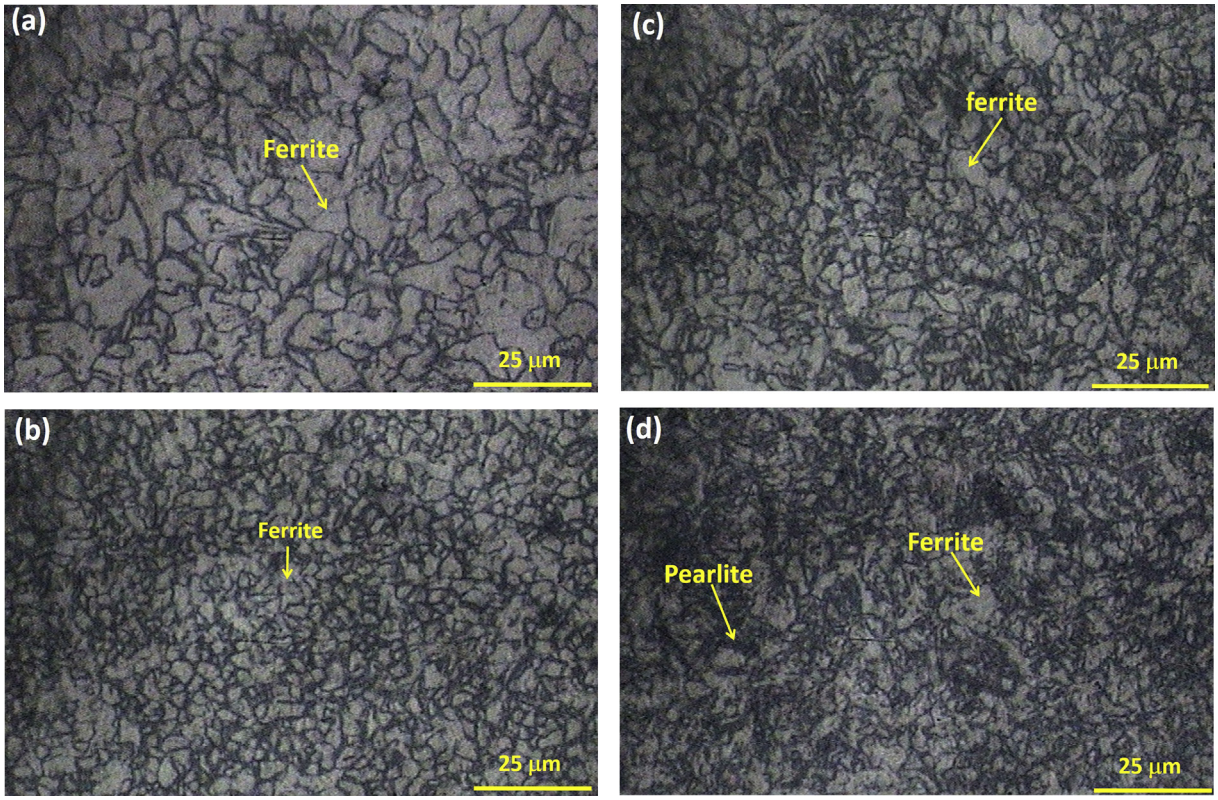

Figure 10. Micro structure of HAZ (a) air weld (b) underwater weld in depth of 2.5 m (c) underwater weld in depth of 5 m (d) underwater weld in depth of 10 m.

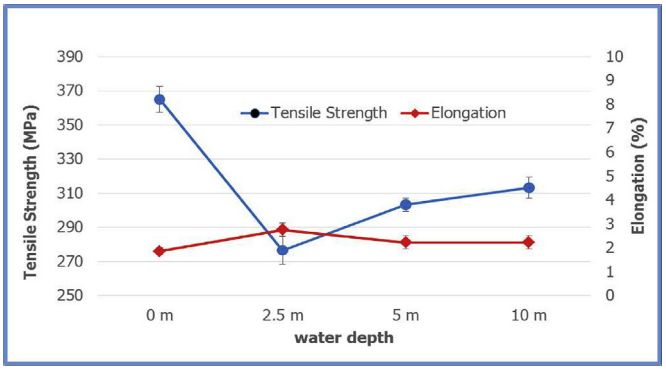

Figure 12. Tensile strength and elongation of underwater welded joint.

3.2.3. Fatigue life

Fatigue life test showed the relationship diagram between cyclic stress and the number of fracture cycles. It is well known as S–N curve or the Wohler diagram. The number of fracture cycles will increase if the cyclic stress decreases [19]. Endurance limit is characterised by the maximum stress that is applied to the material until it fails to unlimited cycles. Figure 14 shows the S–N curve of the underwater and air welded joints. The air welded joint had a higher fatigue resistance than all underwater welded joints. At cyclic stress of 122.8 MPa (37.5% UTS), the air welded joints did not fail up to 2 million cycles, while underwater welded joints in the water depths of 2.5, 5 and 10 m were failed at 1.5 million, 1.6 million and 1.8 million cycles, respectively. The porosities of the underwater weld metal lead to stress concentration which results in initial cracks and subsequent crack propagation. Fatigue strength is determined by the strength of the weakest atomic bonding. It decreases if there are many defects in the material. Cracks will initiate and propagate quickly through the defects. In addition, fatigue strength is also affected by the hardness of material. The higher the material hardness, the higher the material's resistance to crack initiation [20]. Underwater welded joint in water depth of 10 m had higher fatigue resistance than that of 5 m and 2.5 m. The AF structure in the underwater weld metal of 10 m water depth contributed to crack propagation retention. The AF structure has good fatigue resistance, because it improves the mechanical properties by increasing the toughness and tensile strength [21, 22].

The surface fractures of the fatigue tests are shown in Figures 15, 16, 17, and 18. The fatigue fractures of the air welded joints and the

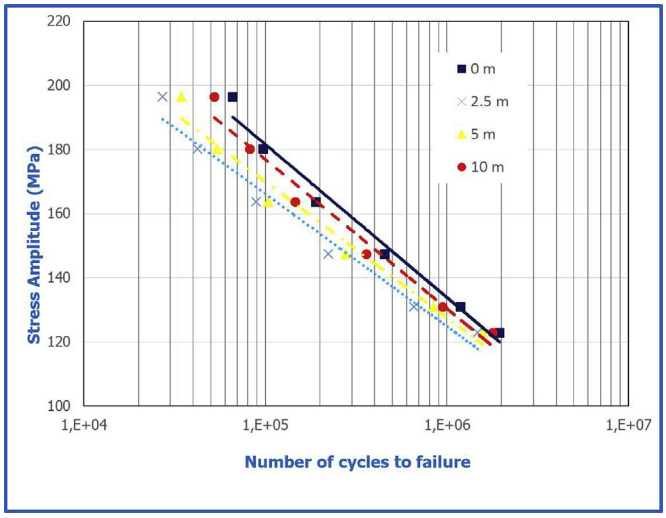

Figure 14. S–N diagram of underwater weld joint.

underwater welded joints occurred in the weld metal. Both weld joints have simillar mode of fracture because of the same structure and bending load. As seen in macrostructures (Figure 7), both weld joints have lack fussion in the joint center in which it is like initial crack and has stress concentration. During rotary bending fatigue loads, bottom and top sides of lack fussion were subjected to the tensile and compressive loads, respectively. Lack fussion of bottom side will be opened due to tensile load, while that of top side will be closed due to compressive load. During rotating, tensile and compressive loads reversed periodically so that the initial crack will propagate until the material experienced the transition between fatigue and over load, and finally static failure occurs. Propagation of crack will be faster when porosities exists [23, 24]. Due to the porosity of the underwater welded joint, as seen in Figures 16, 17, and 18, it has lower fatigue strength than the air welded joint. Besides accelerating the crack propagation, the porosities in weld metal can also be initial crack [25, 26, 27]. Figure 15 shows that crack of the air welded joint grew slowly due to the little porosities. It can be characterised by fine scratching on the fracture surface. Scratching indicated the steps of crack growth due to combination of torsional and bending loads. The scratching was caused by slip between two surfaces after the crack initiation. The coarse scratching indicated the high rate of crack growth

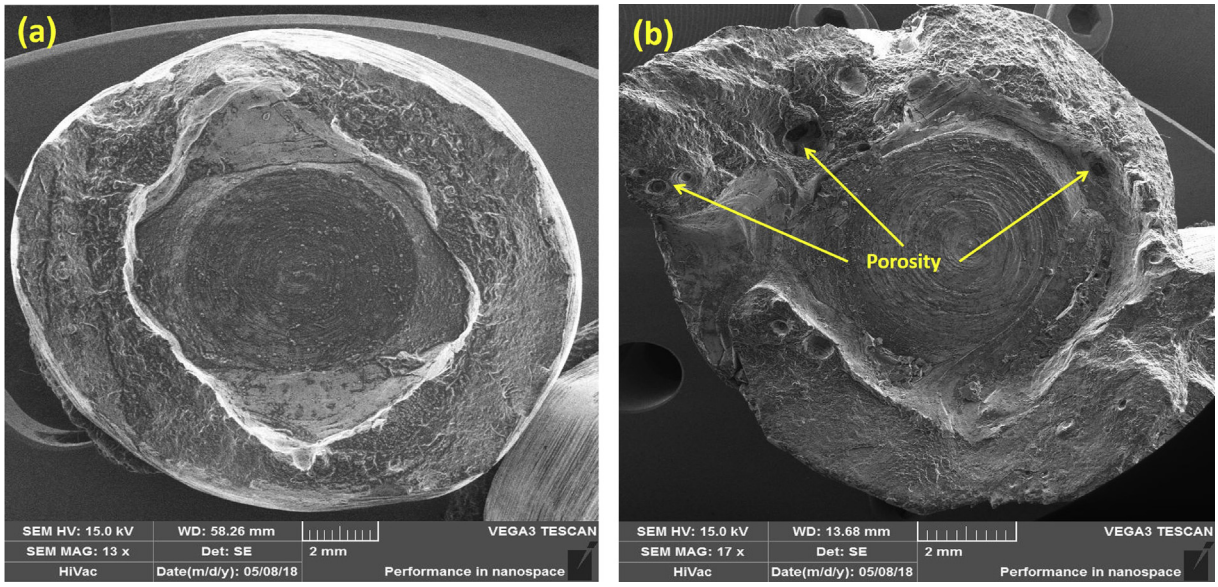

Figure 13. Fracture surface of tensile test for (a) air weld, (b) underwater weld.

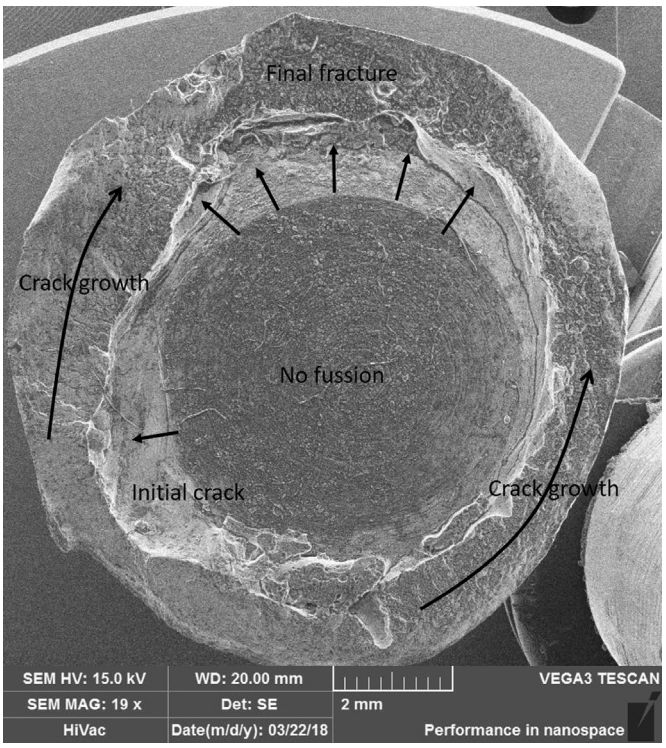

Figure 15. Fracture surface of fatigue test for air weld.

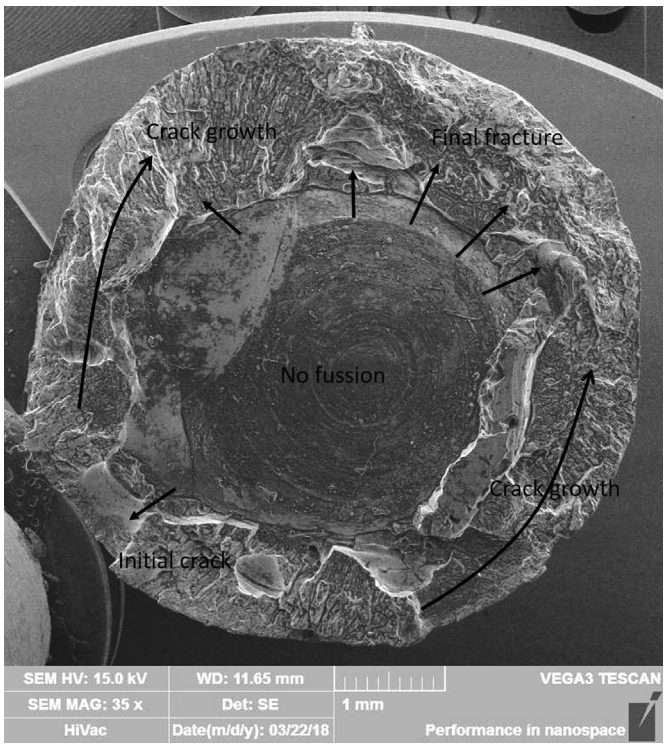

Figure 17. Fracture surface of fatigue test for underwater weld in depth of 5 m.

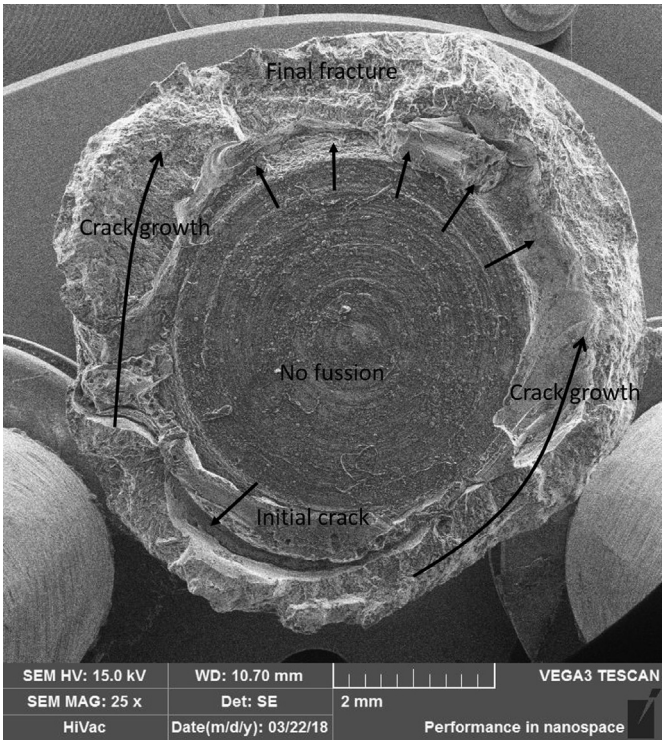

Figure 16. Fracture surface of fatigue test for underwater weld in depth of 2.5 m.

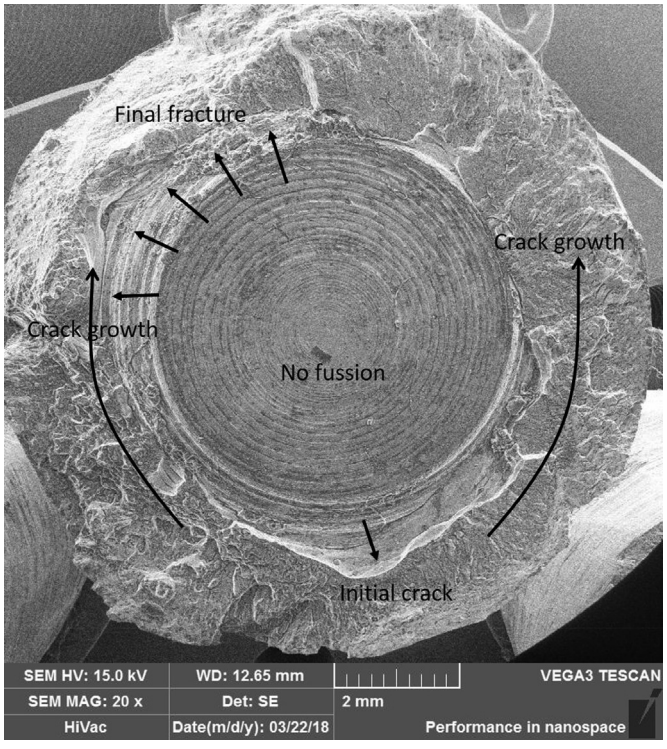

Figure 18. Fracture surface of fatigue test for underwater weld in depth of 10 m.

and it was found in the fracture surfaces of the underwater welded joint in water depth of 2.5, 5 and 10 m. Among them, the finest scratching was found on the fracture surface of underwater welded joints in the water depth of 10 m due to AF content in its weld metal. It led to an increase in the fatigue strength of weld metal. Besides scratching, the striation was also formed in all failure surfaces, as shown in Figures 15, 16, 17, and 18. The striation occurred due to the natural phenomena when the material experienced cyclic loading.

Based on the results and discussion in this study, it is important to improve the fatigue life of underwater welded structures. Unlike in the

air environment, underwater fatigue life enhancement methods and tools are very limited due to the water environment. One of the applicable methods is high-frequency mechanical impact (HFMI). In HFMI, cylinder-shaped indenters are collided against a structure with high frequency. It deformed plastically the structure surface and induced compressive residual stress in the treated area [28]. During underwater treatment, power pack and indenter chamber are placed on the land while indenter gun is directed to the selected underwater welded joint using flexible pipe.

4. Conclusion

The effects of water depth on the fatigue life of underwater wet welded low carbon steel SS400 have been investigated. The new finding of this investigation was the deeper the water, the higher the fatigue and the tensile strength. Based on the microstructure analysis, the number of acicular ferrite structures in weld metal increased as the water depth increased due to the increasing cooling rate which was affected by the surrounding temperature. Due to the presence of porosities, the tensile and fatigue strengths of underwater wet welded joints were lower than those of air welded joint. Porosities were generated by hydrogen gas which was dissolved and trapped in molten metal during the welding process.

Declarations

Author contribution statement

N. Muhayat: Analyzed and interpreted the data; Contributed reagents, materials, analysis tools or data.

Y. A. Matien: Conceived and designed the experiments; Performed the experiments.

H. Sukanto: Performed the experiments; Contributed reagents, materials, analysis tools or data.

Y. C. N. Saputro: Performed the experiments.

Triyono: Conceived and designed the experiments; Analyzed and interpreted the data; Wrote the paper.

Funding statement

This work was supported by Sebelas Maret University through PDUPT Research Grant 2018 with contract No. 474/UN27.21/PP/2018.

Competing interest statement

The authors declare no conflict of interest.

Additional information

No additional information is available for this paper.

References

[1] Y. Zhai, L. Yang, T. He, Y. Liu, Weld morphology and microstructure during simulated local dry underwater FCTIG, J. Mater. Process. Technol. 250 (June) (2017) 73–80.

[2] N. Guo, C. Xu, W. Guo, Y. Du, J. Feng, Characterization of spatter in underwater wet welding by X-ray transmission method, Mater. Des. 85 (2015) 156–161.

[3] X. Di, S. Ji, F. Cheng, D. Wang, J. Cao, Effect of cooling rate on microstructure, inclusions and mechanical properties of weld metal in simulated local dry underwater welding, Mater. Des. 88 (2015) 505–513.

[4] Y. Zhang, C. Jia, B. Zhao, J. Hu, C. Wu, Heat input and metal transfer influences on the weld geometry and microstructure during underwater wet FCAW, J. Mater. Process. Technol. 238 (2016) 373–382.

[5] N. Guo, X. Xing, H. Zhao, C. Tan, J. Feng, Z. Deng, Effect of water depth on weld quality and welding process in underwater fiber laser welding, Mater. Des. 115 (2017) 112–120.

[6] Q.J. Sun, W.Q. Cheng, Y.B. Liu, J.F. Wang, C.W. Cai, J.C. Feng, Microstructure and mechanical properties of ultrasonic assisted underwater wet welding joints, Mater. Des. 103 (2016) 63–70.

[7] H.L. Li, D. Liu, Y.T. Yan, N. Guo, J.C. Feng, Microstructural characteristics and mechanical properties of underwater wet flux-cored wire welded 316L stainless steel joints, J. Mater. Process. Technol. 238 (2016) 423–430.

[8] C. Jia, T. Zhang, S.Y. Maksimov, X. Yuan, Spectroscopic analysis of the arc plasma of underwater wet flux-cored arc welding, J. Mater. Process. Technol. 213 (8) (2013) 1370–1377.

[9] Y. Hu, Y. Shi, K. Sun, X. Shen, Microstructure evolution and mechanical performance of underwater local dry welded DSS metals at various simulated water depths, J. Mater. Process. Technol. 264 (2019) 366–376.

[10] J. Feng, J. Wang, Q. Sun, H. Zhao, L. Wu, P. Xu, Investigation on dynamic behaviors of bubble evolution in underwater wet flux-cored arc welding, J. Manuf. Process. 28 (2017) 156–167.

[11] C. Pandey, N. Saini, M.M. Mahapatra, P. Kumar, Hydrogen induced cold cracking of creep resistant ferritic P91 steel for different diffusible hydrogen levels in deposited metal, Int. J. Hydrogen Energy 41 (39) (2016) 17695–17712.

[12] M.S. Mohsenzadeh, M. Mazinani, On the yield point phenomenon in low-carbon steels with ferrite-cementite microstructure, Mater. Sci. Eng. A 673 (2016) 193–203.

[13] W. Gao, D. Wang, F. Cheng, X. Di, C. Deng, W. Xu, Microstructural and mechanical performance of underwater wet welded S355 steel, J. Mater. Process. Technol. 238 (2016) 333–340.

[14] I.I. Boyadjiev, P.F. Thomson, Y.C. Lam, Computation of the diffusional transformation of continously cooled austenite for predicting the coefficient of thermal expansion in the numerical analysis of thermal stress, ISIJ Int. 36 (11) (1996) 1413–1419.

[15] Y. Zhao, Q. Wang, H. Chen, K. Yan, Microstructure and mechanical properties of spray formed 7055 aluminum alloy by underwater friction stir welding, Mater. Des. 56 (2014) 725–730.

[16] S.H. Park, C.S. Lee, Relationship between mechanical properties and high-cycle fatigue strength of medium-carbon steels, Mater. Sci. Eng. A 690 (2017) 185–194.

[17] M. Mosallaee, J. Hydari, S. Ghassemy, A. Mashreghee, Effect of E8010-P1 electrode composition on the weld metal properties, Int. J. Pres. Ves. Pip. 111–112 (2013) 75–81.

[18] Y. Yin, X. Yang, L. Cui, F. Wang, S. Li, Material flow influence on the weld formation and mechanical performance in underwater friction taper plug welds for pipeline steel, Mater. Des. 88 (2015) 990–998.

[19] D. Tchoffo Ngoula, H.T. Beier, M. Vormwald, Fatigue crack growth in cruciform welded joints: influence of residual stresses and of the weld toe geometry, Int. J. Fatig. 101 (2017) 253–262.

[20] J.D. Bressan, D. Kohls, Rotating bending fatigue tests of PH-42 steel plasma Nitrided, in: 13th International Conference on Fracture," June 16–21, Beijing, China, 2013.

[21] W.L. Costin, O. Lavigne, A. Kotousov, A study on the relationship between microstructure and mechanical properties of acicular ferrite and upper bainite, Mater. Sci. Eng. 663 (2016) 193–203.

[22] X.J. Yan, D.Z. Yang, M. Qi, Rotating-bending fatigue of a laser-welded superelastic NiTi alloy wire, Mater. Char. 57 (1) (2006) 58–63.

[23] A.R. Arias and A.Q. Bracarense, Fatigue crack growth rate in underwater wet welds: out of water evaluation, Weld. Int. 31 (5), 2017

[24] A.R. Arias, A.Q. Bracarense, Fatigue crack growth assessment in underwater wet welds, Weld. J. 96 (2017) 287–294.

[25] M.J. Khameneh, M. Azadi, Evaluation of high-cycle bending fatigue and fracture behaviors in EN-GJS700-2 ductile cast iron of crankshafts, Eng. Fail. Anal. 85 (2018) 189–200. December 2017.

[26] C. Pandey, M.M. Mahapatra, P. Kumar, N. Saini, A. Srivastava, Microstructure and mechanical property relationship for different heat treatment and hydrogen level in multi-pass welded P91 steel joint, J. Manuf. Process. 28 (2017) 220–234.

[27] N. Guo, D. Liu, W. Guo, H. Li, J. Feng, Effect of Ni on microstructure and mechanical properties of underwater wet welding joint, Mater. Des. 77 (2015) 25–31.

[28] D. Andud, M.F. Mat, Y.H.P. Manurung, S. Saidin, N. Nordin, N. Muhammad, M. Laitner, Fatigue life enhancement of transverse and longitudinal tjoint on offshore steel structure HSLAS460G2+M using semiautomated GMAW and HFMI/PIT, MATEC Web Conf. 269 (2019), 06001.